DATA 61
www.csiro.au

Spark Evaluation

Comparison of Wildfire Rate of Spread Models Implemented within the Spark Framework to Historical Reconstructions of Wildfire Events.

William Swedosh, James Hilton

Draft A

26/8/2016

Data 61, CSIRO

Draft A: All simulations used spark-batch release revision 38086, Spark framework version 0.7.1

Contents

Figures

Acknowledgments

We wish to thanks a number of researchers and agency staff for help and data for this project: Andrew Sullivan and the team in the Land and Water division at CSIRO for invaluable guidance in fire science, Stuart Matthews at New South Wales Rural Fire Service for providing data for New South Wales fires and Robert Fawcett and Jeff Kepert from the Bureau of Metrology for providing metrological data sets for historical fire events.

1 Introduction

1.1 Overview

The aim of this project is to create, maintain and grow a standard data set of historical fire events which can be used in an ongoing effort to improve fire prediction through the Spark framework. This 'standard input stack' of fire simulations can be used to validate fire models, test new rate of spread models and check the Spark framework for systematic errors before new versions are publically released. Furthermore, the standard input stack is intended to be publically available, allowing researchers using the Spark framework a starting point for full scale fire simulations. The stack is intended to grow as new historical events are added, and the results from the comparison are intended to improve over time as new rate of spread models, behaviour models and computational methods are developed.

The project is *not* intended to give a best fit to historical fire models, or to detail a set of tweaks required to match a simulation with a particular fire event. Rather, the project is intended as a snapshot of the model performance for using the newest research and best current modelling techniques. As these are improved and updated the results will be updated accordingly. Similarly, as better input data becomes available (such as fuel and meteorological conditions) the results will be updated using the newer data. The report provides a comparison of model performance, as well as highlighting shortcomings in the current state of the art to identify areas for future improvement.

1.2 Spark

The Spark framework is a fully configurable fire propagation system allowing rate-of-spread models for any fuel type to be easily implemented. The system includes a range of plug-in packages including generation of wind fields, topographic correction of wind fields, spot fire models and road/transmission line crossing.

The system is based on a level set propagation model, allowing simulation of any number of distinct fire perimeters, multi-front interaction and coalescence as the fire evolves. The method is parallelised on GPU architecture, enabling simulations to run much faster than real time.

The framework is based on the CSIRO developed Workspace, a computational workflow tool. Each element of wildfire simulation, such as reading input data, running the simulation and outputting data can be fully customised within this workflow environment. The system has integrated geospatial support, image analysis, scripting, database, and provenance reporting, making Spark compatible with any standard data types.

Spark allows any number of input data layers to be used and combined in any way within rate-of-spread calculations. The model is raster-based, where each cell can be classified by fuel type and use a different rate-of-spread model. The system handles all temporal and spatial interpolation of input data, allowing the user to define rate-of-spread models in a clear and straightforward manner.

1.3 Comparison Wildfires

The wildfires used for comparison are listed below:

	Name	State	Year
1.	Lithgow, state mine	NSW	2013
2.	Kilmore East	VIC	2009
3.	Giblin River	TAS	2013
4.	Forcett-Dunalley	TAS	2013
5.	Mount Cooke	WA	2003
6.	Wangary	SA	2005
7.	Pickering Brook	WA	2005

For each of these cases the best available input data sets were used. The input data sets included land classification, fuel conditions and metrological data. The input data used in each case is detailed in the following sections. For situations were no input data was available the methodology used to construct required inputs is detailed. Each of the cases was simulated for time periods between 4 to 40 hours.

2 Model Inputs

This section describes the input data to the simulations and the spread rate models used for each of the cases.

2.1 Meteorological Input Data

Wind and weather data is the most important information required for a bushfire simulation. For several of these cases only point source metrological data was available from an automated weather station (AWS). For others, however, gridded reconstructed metrological data is available. This data was available in the following forms:

- Time series values from Bureau of Meteorology (BoM) AWS. This data is a point source time series that is usually recorded at intervals of 30 minutes or one hour. Wind speed and direction, surface temperature, relative humidity and dew point temperature (among others) are available from the supplied comma separated variable (CSV) files. This data is highly accurate, however, it is recorded at a fixed point, usually in different topography many kilometres from the fire.
- Gridded NetCDF datasets. This data is three dimensional (2D space and varies with time). This is generated as a prediction or as a reconstruction. Predicted data may not be what was observed as it is a forecast from a model. Hindcast reconstructions calibrated to AWS data are the most accurate gridded datasets available.

The framework contains a sub-module for down sampling and correcting wind flow over topography. This is currently undergoing testing and validation, and was not used in the current version of this study.

2.2 Initial Fire Conditions

The initial position and size of the fire front as the start of the simulation can either be defined as a set of circular point sources (specifying locations, radii and start times), or using a geo-referenced raster or shape file dataset. The simulation resolution is set when specifying the initial fire conditions.

2.3 Geospatial Input Data

The two main geospatial input groups are fuel data and terrain data. Different rate-of-spread models require different fuel data layers. Terrain data is common to all rate of spread models and consisted of:

1. Topographic digital elevation model (meters above a datum such as AHD). This was sourced from Geoscience Australia Digital Elevation Data[1].
2. Land classification data for defining the cover type and hence rate-of-spread model to be used. This data was sourced from Catchment Scale Land Use of Australia[2] (classifications from Australian Land Use and Management Classification[3]) or the TasVeg data set[4].

Internal classifications were assigned as:

Class id	Land type	Rate of spread model
0	Unburnable (water/rock)	None
1	Grassland	CSIRO grassland
2	Forest	Dry Eucalypt
3	Urban	Proportional to wind
4	Moorland	Buttongrass moorland

The methods and initialisation models used to convert various land use maps into classification layers are reported in Appendix A . Results from the simulations were projected onto a base satellite map image (Bing Aerial with labels) in QGIS.

Geospatial data layers can be specified in a number of ways:

- A constant value specified over the entire simulation domain,
- A two dimensional map with spatially varying levels,
- A three dimensional map with spatially and temporally varying levels,
- A model defined in an initialisation stage specifying the two-dimensional values over the domain.

The layers in each of the test cases used one of the above, depending on data availability.

All of the input data layers are required to be converted into a Cartesian projection (for example, Mercator or conical) before being used in the solver. The conversion is carried out within the framework from an Open Geospatial Consortium (OGC) well-known text (WKT) string specifying the projection parameters.

[1] Digital Elevation Data: http://www.ga.gov.au/scientific-topics/national-location-information/digital-elevation-data

[2] Catchment Scale Land Use of Australia: https://www.data.gov.au/dataset/catchment-scale-land-use-of-australia-update-march-2014

[3] Australian Land Use and Management Classification: http://www.agriculture.gov.au/abares/aclump/land-use/alum-classification-version-7-may-2010

[4] TASVEG: http://dpipwe.tas.gov.au/conservation/flora-of-tasmania/monitoring-and-mapping-tasmanias-vegetation-(tasveg)/tasveg-the-digital-vegetation-map-of-tasmania

2.4 Fire Spread Rate Models

The fire spread rate models used in the comparison simulations are described in this section.

2.4.1 Grasslands

The CSIRO grassland model[5] (Cheney et al. 1998) was used for all grassland areas within the domain. The undisturbed, cut/grazed/trampled, and eaten out variants (Cruz et al. 2015b) were implemented either over the whole domain or within specific regions. Dead fuel moisture content and curing level were required as inputs into this model.

Curing

The curing coefficient was calculated using the equation proposed by Cruz et al. (2015a). Sensitivity analyses could be conducted in future studies where the curing coefficient is calculated using the equation proposed by Cheney (1998). This may reduce the simulated burn areas as Cheney's curing model predicts slower spread rates for the same curing level.

Fuel moisture content

Fuel moisture content was estimated from McArthur (1966), using surface temperature and relative humidity as inputs. Future work will involve estimating the dead fuel moisture content based on recent rainfall, sun exposure, time of year, topography, temperature, relative humidity and other factors. Integration of remote sensing is also being investigated to give spatial maps of moisture content.

2.4.2 Dry Eucalypt Forest

The dry eucalypt or VESTA model[6] was used for all forest areas within the domain. The fuel hazard score version of the model is implemented. Dead fuel moisture content and fuel hazard scores were required as inputs into this model.

Fuel hazard scores

The fuel hazard scores are surface fuel hazard (FHSs, 0-4), near surface fuel hazard (FHSns, 0-4) and near surface height (Hns, cm). Fuel Hazard Scores were defined in the simulations either from spatial maps and calculation from fuel ages.

For calculation from fuel ages, Eq. (1) and Eq. (2) give exponential and hyperbolic relationships between the hazard score and the fuel age (Gould *et al.* 2011). These equations are assumed to be reasonable estimates up to a fuel age of approximately 25 years:

$$h_{exp} = a * (1 - \exp(-k * A)) \quad (1)$$

[5] Available from: http://research.csiro.au/spark/resources/model-library/csiro-grassland-models/

[6] Available from: http://research.csiro.au/spark/resources/model-library/vesta/

$$h_{hyp} = (a * A)/(b + A) \quad (2)$$

Where *h* is the hazard score and *a*, *b* and *k* are different fitting constants for FHSs, FHSns and Hns, and *A* is the fuel age. The fitting constants also depend on whether the under story layer is considered tall shrub or low shrub. These equations were implemented in the initialisation model of Spark to build a spatial map of the fuel parameters.

Fuel moisture content

Fuel moisture content levels were estimated from surface temperature and relative humidity values using Gould et al. (2007) and Matthews et al. (2010). Other fuel moisture models such as Viney and Hatton (1989), and Viney (1992) could be used for sensitivity analysis. Integration of remote sensing data is also being investigated to give spatial maps of moisture content.

2.4.3 Buttongrass Moorlands

The Marsden-Smedley and Catchpole (1995) model[7] was used for all moorland areas within the domain. Fuel moisture content and fuel age were required as inputs into this model.

Fuel age

Fuel age was defined either using a spatial map or a constant value over the domain.

Fuel moisture content

Fuel moisture content levels were estimated from surface temperature and relative humidity values using Marsden-Smedley and Catchpole (2001).

2.4.4 Urban

In lieu of any existing empirical models, a linear rate-of-spread was used in urban areas. The fire spread rate (m/s) was assumed to be 0.8% of the wind speed (in km/h). Due to the uncertain fuel loads and environment in urban areas, future sensitivity analyses could be conducted with varying spread rates. Depending on the simulation region, this may or may not be considered to be critical as the urban areas are often outweighed by the grass and forest areas in the simulated regions, but the wildfires sometimes occur on the urban fringe or near major infrastructure such as highways.

Ongoing research is required in this field. Some urban classifications such as mid-sized roads may easily crossed if there is adjacent eucalypt forest with significant short range spotting. Other urban classifications such as large highways or large concreted areas with no vegetation may in some cases be able to stop a flanking or backing fire or a low intensity grass fire and such be treated as un-burnable.

[7] Available from: http://research.csiro.au/spark/resources/model-library/buttongrass-moorlands/

2.4.5 Slope Effects

The effect of slope on fire spread rate was included using McArthur's rule of thumb (McArthur 1967). This rule states that the head fire spread rate doubles for every 10° of parallel incline for a slope range from 0° to 20°. For slopes above 20°, a speed gain for 20° is assumed. For negative slopes, the CSIRO Kataburn model (Sullivan et al. 2014) is applied. For slopes below -20°, a speed reduction factor of approximately one half is applied. Future work will investigate the sensitivity to the slope model, for example making the terrain un-burnable if there is a slope above a given threshold value (as some steep terrains grow little to no vegetation). Various two dimensional slope models can also be implemented within the framework. A scalar method (Sharples 2008) was implemented in the analyses presented in this report.

The slope model was applied to all vegetation types. Slope effects have not been applied to urban classifications as these regions can be a combination of variable, discontinuous or un-burnable fuels.

2.5 Resolution

Spark simulations can be run at different resolutions or grid sizes. A grid size of 30 metres was used for the simulations in this report. Increasing the grid size would decrease the computational time for the simulation to be conducted, however smaller scale features in topography and land cover may not be captured as accurately. Decreasing the grid size captures smaller scale details, but increases the computational time for the simulation to be conducted. A grid size of 30 m was chosen as it matched the highest resolution national topography data available (one arc second from Geoscience Australia) as well as the common Landsat 8 remote sensing data sets.

3 Lithgow State Mine Case

3.1 Background

The Lithgow State Mine bushfire started on 16 October 2013 and burned in New South Wales until 25 October 2013. The fire was caused by a training exercise being carried out by the Australian Defence Force. The fire travelled the furthest distance and the fastest speed on 17 October 2013, burning through a large area of dry eucalypt forest.

The fire was simulated for a period of just over 9 hours on 17 October 2013.

3.2 Model Parameters

DATA TYPE	DATA SOURCE
Meteorological Data	1. Mount Boyce AWS, ID: 063292, Lat/Long: -33.62, 150.27, Elevation: 1080 m 2. BoM gridded data
Other Available Meteorological Data	Bathurst Airport AWS
Land Use Classification	CLUM for data, initialisation model in Appendix A.1 was used for classification grid mapping
Topography	GA 30m raster (AHD)
Curing Level	Constant value of 80% was assumed based on time of year
Fuel Loads	A constant fuel age of 20 years was assumed for the simulation. Fuel hazard scores were then estimated from growth curves.
Initial Fire for Simulation	Shapefile of reconstructed fire fronts starting at 11:59 on 17 October 2013
Simulation End Time	21:15 on 17 October 2013
Output Comparison	Observed / reconstructed fire front at 21:15 on 17 October 2013

3.3 Results and Discussion

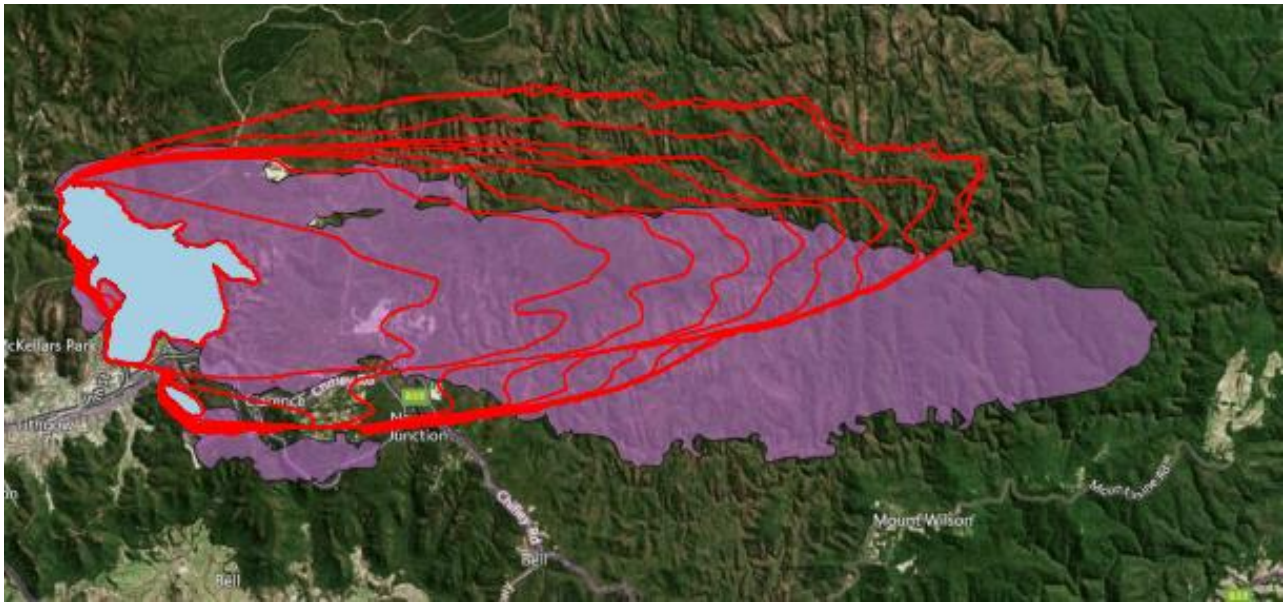

Figure 1 – Hourly isochrones of Lithgow State Mine simulation shown in red. Mount Boyce AWS data used for weather inputs. Initial fire shown in blue. Reconstructed fire at 21:15 is shown in purple for comparison.

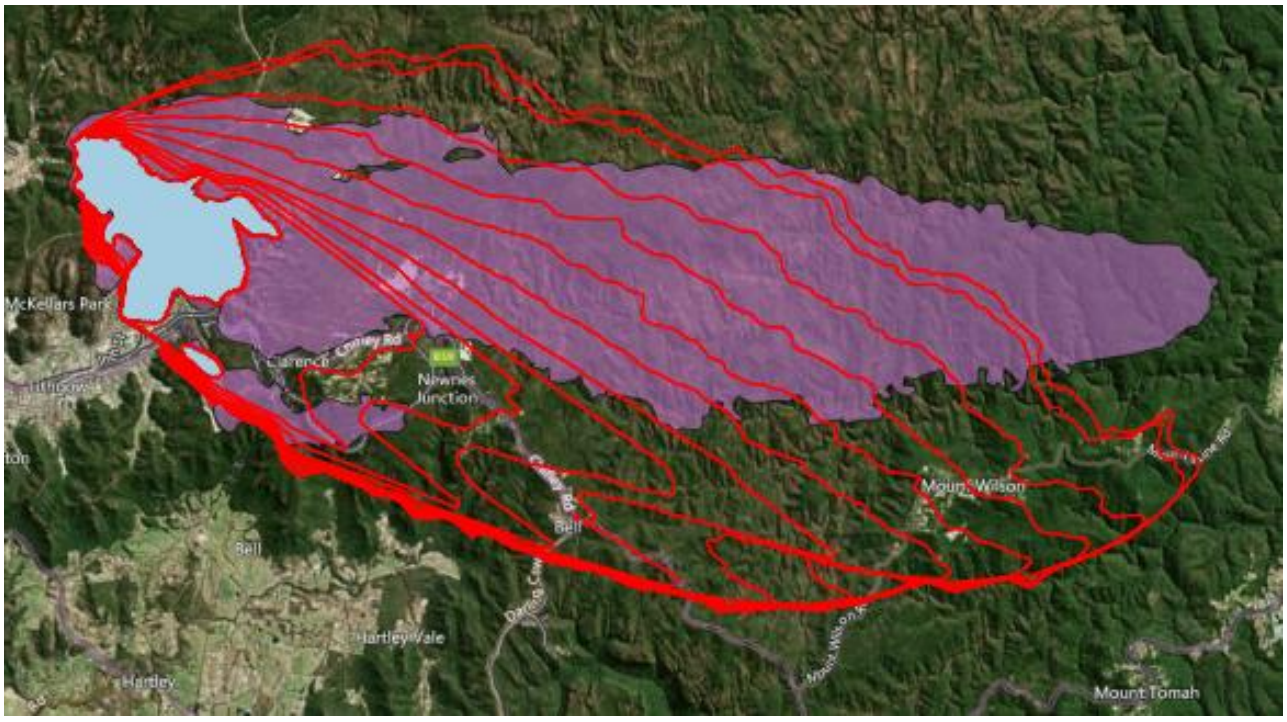

Figure 2 – Hourly isochrones of Lithgow State Mine simulation shown in red. Gridded NetCDF data used for weather inputs. Initial fire shown in blue. Reconstructed fire at 21:15 is shown in purple for comparison.

The Lithgow case provides a reasonable match over a long simulation duration but highlights the sensitivity of the predictions to the meteorological data used. Figure 1 shows the simulated fire using the Mount Boyce AWS meteorological data while Figure 2 shows the simulated fire using the gridded data.

3.3.1 Mount Boyce meteorological data

The simulation based on AWS data values predicts a similar burn area to the reconstructed fire. However, the simulation over predicts to the north and under predicts to the east. The simulation also over predicts the burned area to the south of the main fire near the start of the simulation. Possible reasons for these differences include:

1. Unmodified weather data from the Mount Boyce AWS was used, which was approximately 20 km away from the fire. This potentially resulted in higher relative humidity, and hence lower spread rates than were actually achieved. The wind direction from the AWS appears to be south-westerly compared to the westerly wind direction indicated by the fire scar during later times in the simulation.
2. A spotting model was not included in the simulation. Spotting was present during the actual fire as evidenced by the two initial burn areas. Including such a model could increase the easterly rate of spread.
3. The fire being actively supressed at the Southern edge of the fire near the start of this simulation (which was not simulated) to protect the urban population and urban fringe.

3.3.2 Gridded meteorological data

The simulation based on BoM gridded data predicts a larger burn area compared to the reconstructed fire. The simulation does predicts a much greater southern extent than the reconstruction. Possible reasons for these differences include:

1. Unmodified NetCDF weather model data was used. This data may not have matched the ground conditions during the fire. The gridded wind direction appears to north-westerly, rather than the westerly wind direction from the fire scar near the middle and the end of the simulation.
2. A spotting model was not included in the simulation. Spotting was present during the actual fire as evidenced by the two initial burn areas. This could increase the easterly rate of spread.
3. The fire being actively supressed at the Southern edge of the fire near the start of this simulation (which was not simulated).

Future work could investigate inclusion of a spotting model, accounting for suppression at the urban fringe and modifying weather input based on topography to improve the model predictions.

4 Kilmore East Case

4.1 Background

The Kilmore East bushfire started on 7 February 2009 and burned in Victoria until it was contained in early March. It was the largest fire out of the Black Saturday bushfires. The fire was started by a power line and burned the fastest and most intensely on 7 February 2009. Further background information is contained in Cruz et al. (2012).

The fire was simulated for a period of 4 hours on 7 February 2009.

4.2 Model Parameters

DATA TYPE	DATA SOURCE
Meteorological Data Used	Wallan (Kilmore Gap) AWS, ID: 088162, Lat/Long: -37.38, 144.97, Elevation: 528 m
Other Available Meteorological Data	None identified
Land Use Classification	CLUM for data, initialisation model in Appendix A.1 was used for classification grid mapping
Topography	GA 30m raster (AHD)
Curing Level	Constant value of 100% was assumed based on time of year
Fuel Loads	A constant fuel age of 15 years was assumed for the simulation. Fuel hazard scores were then estimated from growth curves.
Initial Fire for Simulation	Shapefile at 13:00 on 7 February 2009 based on Cruz et al (2012)
Simulation End Time	17:00 on 7 February 2009
Output Comparison	Observed / reconstructed fire fronts at 14:00, 16:00 and 17:00 on 7 February 2009

4.3 Results and Discussion

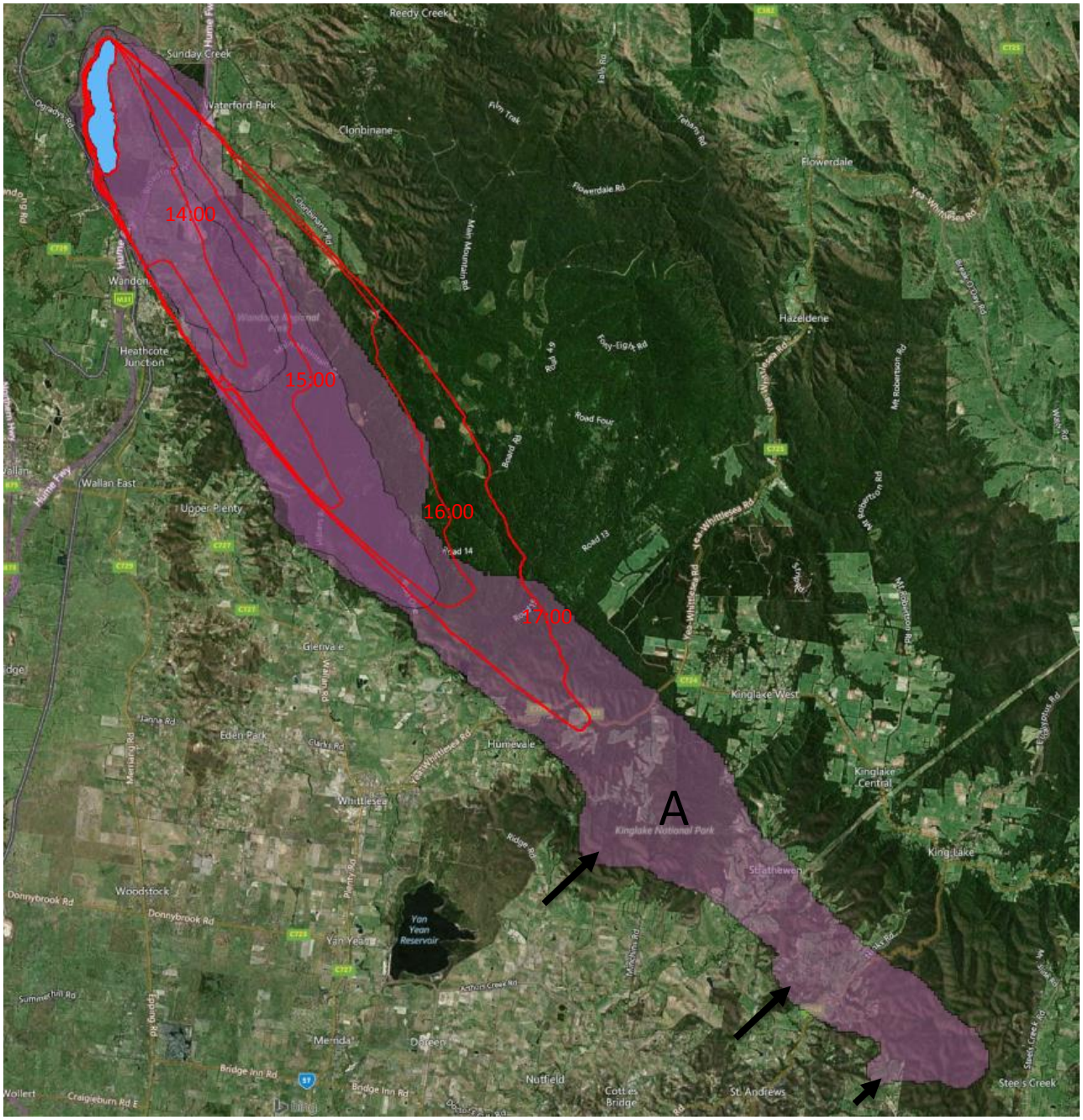

Figure 3 – Hourly isochrones of Kilmore East simulation shown in red, first isochrones at 14:00. Initial fire shown in blue. Reconstructed fires at 14:00, 16:00 and 17:00 are shown in purple for comparison. Note that there is no reconstruction at 15:00.

The Kilmore case shows good agreement in the extent of the predicted fire for the first few hours of the simulation. However, the simulation results in a significant under prediction of the burned area at 17:00 (see Figure 3, area 'A'). This is most likely due to the following factors:

1. A spotting model was not included in the simulation. It was reported that significant long range spotting of several kilometres occurred during the afternoon of the fire. Some of these break outs can be seen on the southern flanks of reconstruction (arrows in Figure 3).

2. Unmodified weather data from the Kilmore Gap AWS was used. As the fire propagated to the south east the head of the fire moved further from the weather station used for input data. This may have resulted in different wind speeds at the head of the fire to that used in the model.

To attempt to better correlate with actual fire observations, adjustments could be made to the input weather data including increasing the wind speed. Future modelling could also include long range spot fires ignited from recorded breakout positions.

5 Giblin River Case

5.1 Background

The Giblin River bushfire started from a lightning strike on 3 January 2013 and burned in Tasmania until 22 January 2013. The fire burned through many different types of vegetation and resulted in a final burn area of 45,124 ha. Further background information is contained in Marsden-Smedley (2014).

The fire was simulated for a period of just over 25 hours starting on 3 January 2013.

5.2 Model Parameters

DATA TYPE	DATA SOURCE
Meteorological Data Used	Scotts Peak Dam AWS, ID: 097083, Lat/Long: -43.04, 146.27, Elevation: 408 m
Other Available Meteorological Data	Low Rocky Point AWS
Land Use Classification	TASVEG for data, initialisation model presented in Appendix A.2 for classification grid mapping
Topography	GA 30m raster (AHD)
Curing Level	Constant value of 80% was assumed based on time of year
Fuel Loads	A constant fuel age of 15 years was assumed for the simulation. Fuel hazard scores were then estimated from growth curves.
Initial Fire for Simulation	Assumed to be at 145.796 E, 43.009 S (within 2km from 401950, 5237070 (GDA94/55)) with a radius of 200 m at 15:00 on 3 January 2013 based on Marsden-Smedley (2014)
Simulation End Time	16:15 on 4 January 2013
Output Comparison	Observed / reconstructed fire front at 16:15 on 4 January 2013

5.3 Results and Discussion

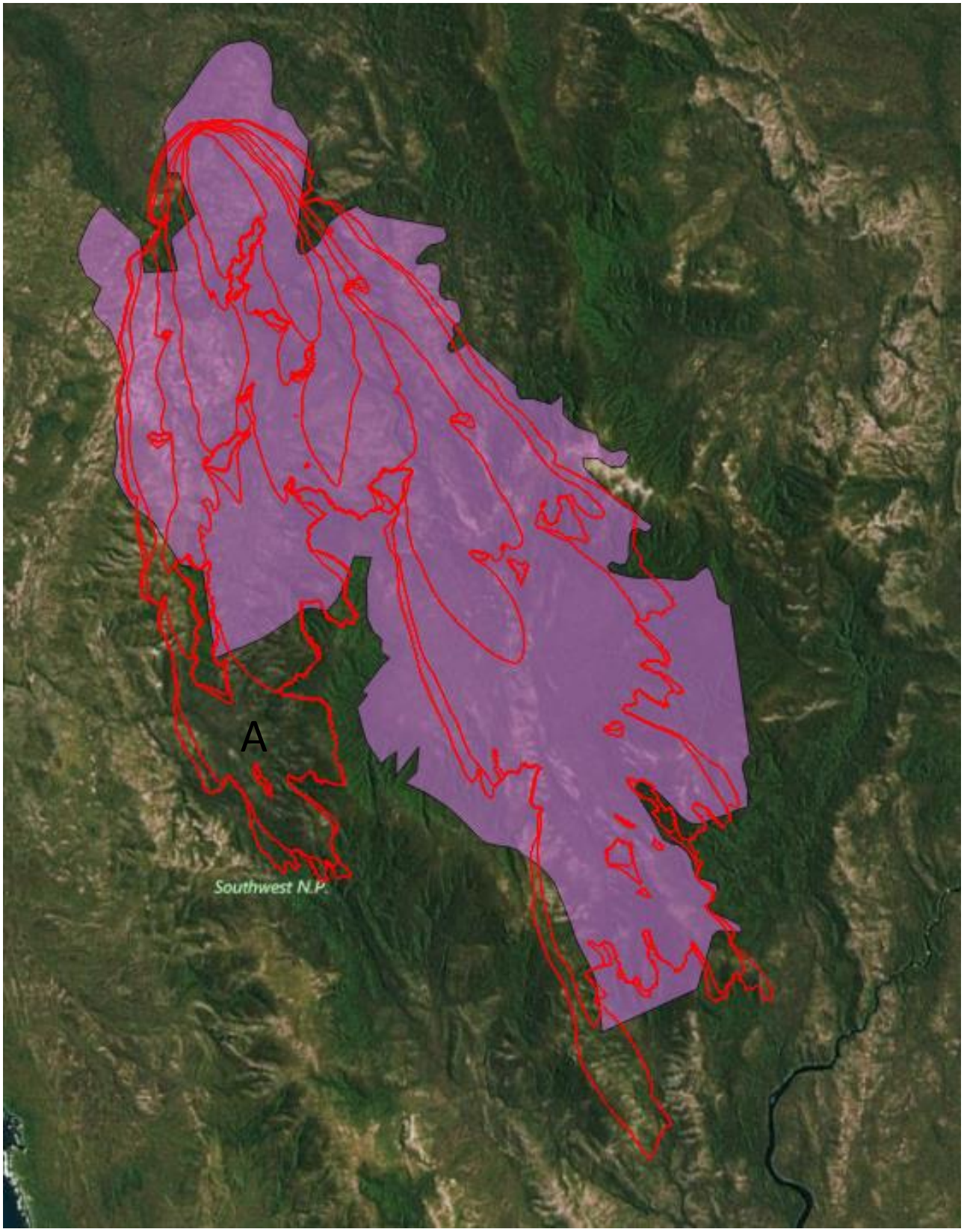

Figure 4 – Four-hourly isochrones of Giblin River simulation shown in red, first isochrone at 19:00 on January 3. Reconstructed fire at 16:15 on January 4 is shown in purple for comparison.

The Giblin river case resulted in good overall size and extent agreement with the reconstructed fire at the south east head fire. However, there was an over prediction of the burned area on the south west flank (see Figure 4, area 'A'). Differences may be due to the following factors:

1. The TASVEG dataset contained many different vegetation types, even in the relatively small area of the fire. For the simulation these were classified to known rate of spread models: dry eucalypt forest, grass land, moorlands, or un-burnable. These assumptions are likely to have introduced errors into the overall rate of spread, for example mapping wet eucalypt forest to a dry eucalypt rate of spread as well as treating rainforest as un-burnable.
2. A constant fuel age was assumed for the simulation. A detailed fuel age or fuel load map may improve the simulation through more accurate fuel load values.
3. The ignition of the fire is only known to be within an area of 2km radius. Due to the multiple land classifications within the ignition region the simulation is sensitive to the start location.

The inclusion of calibrated and published spread rate models for more of the vegetation types present, such as rain forest, scrub and highlands, as well as a fuel load or fuel age map may provide a better match to the reconstructed fire extent. An initialisation model could also be developed which estimates or adjusts fuel loads based on the elevation, slope and aspect of the terrain.

6 Forcett-Dunalley Case

6.1 Background

The Forcett-Dunalley bushfire started east of Hobart on 3 January 2013 and burned until contained on 18 January 2013. The fire burned through several different vegetation types and significant spotting was observed at times. The final burn area of the fire was 23,960 ha. Further background information is contained in Marsden-Smedley (2014).

The fire was simulated for a period of just over 24 hours starting on 3 January 2013.

6.2 Model Parameters

DATA TYPE	DATA SOURCE
Meteorological Data Used	Dunalley (Stroud Point) AWS, ID: 094254, Lat/Long: -42.90, 147.79, Elevation: 12.4 m
Other Available Meteorological Data	Hobart Airport AWS
Land Use Classification	TASVEG for data, initialisation model presented in Appendix A.2 for classification grid mapping
Topography	GA 30m raster (AHD)
Curing Level	Constant value of 80% was assumed based on time of year
Fuel Loads	A constant fuel age of 15 years was assumed for the simulation. Fuel hazard scores were then estimated from growth curves.
Initial Fire for Simulation	Assumed to be at 147.6751 E, 42.8065 S (within 25m from 555195, 5260448 (GDA94/55)) with a radius of 100 m at 14:00 on 3 January 2013 based on Marsden-Smedley (2014)
Simulation End Time	14:30 on 4 January 2013
Output Comparison	Observed / reconstructed fire front at 14:30 on 4 January 2013

6.3 Results and Discussion

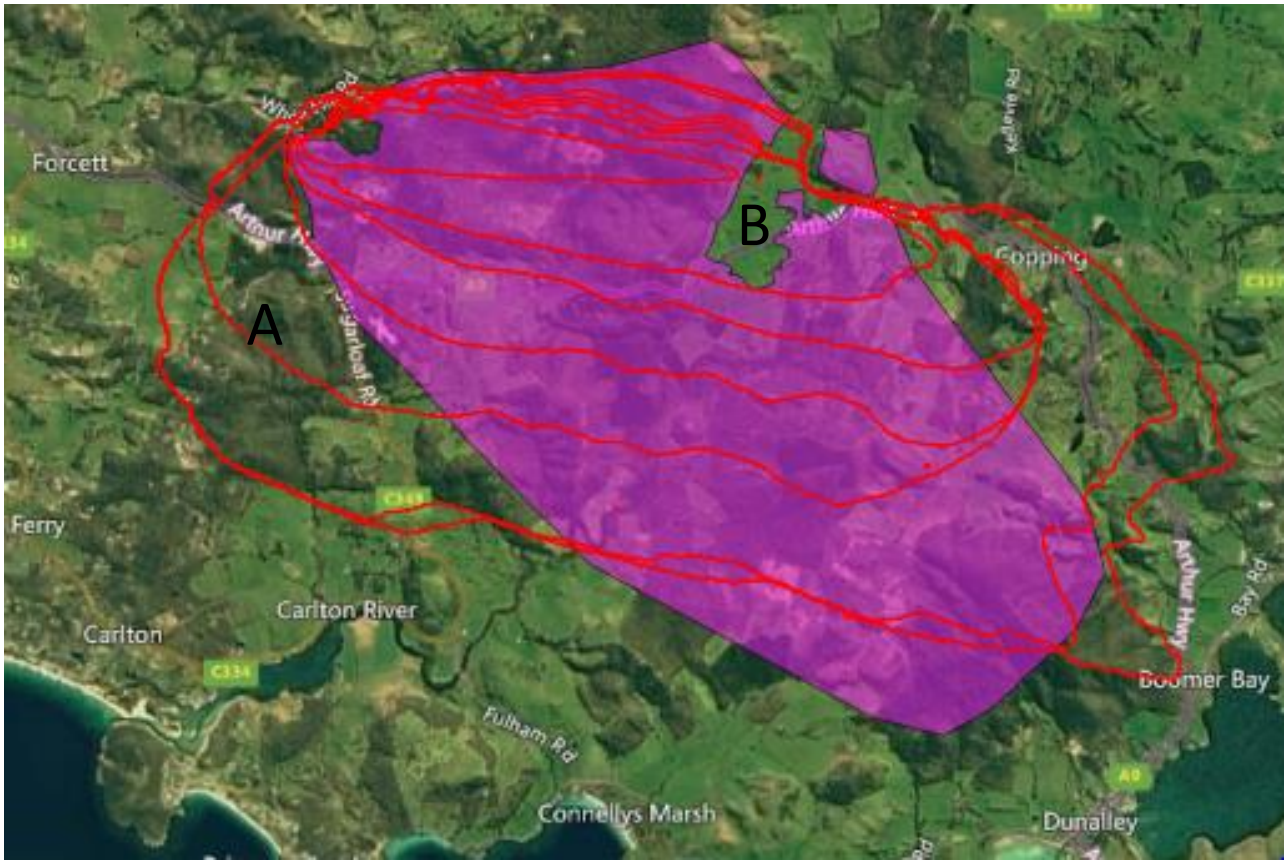

Figure 5 – Four-hourly isochrones of Forcett-Dunalley simulation shown in red, first isochrone at 18:00 on January 3. Reconstructed fire at 14:30 on January 4 is shown in purple for comparison.

The Forcett-Dunalley simulation had reasonable overall agreement between the extent and size of the reconstructed burn area and the simulation. The simulation resulted in an over prediction of the burned area of the south west and north east flanks and an under prediction of the burned area at the south east of the fire (see Figure 5). This may be due to the following factors:

1. The TASVEG dataset contained many different vegetation types, even in the relatively small area of the fire. For our simulation, these were all classified into known rate-of-spread models: dry eucalypt forest, grass land, moorlands, or un-burnable. Mappings were based on 11 vegetation groups (given in Appendix A.2).
2. A constant fuel age was assumed for the simulation. A detailed fuel age or fuel load map may improve the simulation through more accurate fuel load values.
3. Unmodified weather data from the Dunalley AWS was used, which was some distance from the start fire. This is likely to have resulted in slightly different wind speeds and directions that at the head of the fire.
4. The reconstructions show the fire may have been controlled along the western flank (Arthur Highway and Sugarloaf Rd). This was not included in the simulation and may have resulted in a significant reduction in the burn area 'A'.

5. Farmland area towards the north east (area ‘B’) appeared to be bare earth in satellite images. This was not included in the simulation and would have resulted in a reduction of burned area to the east.

The inclusion of calibrated and published spread rate models for more of the vegetation types present, such as agricultural lands, plantations and scrub, as well as a fuel load or fuel age map may improve match between the simulation and reconstruction. Modifying weather inputs may also improve the simulation through more accurate wind conditions.

7 Mount Cooke Case

7.1 Background

The Mount Cooke bushfire started from a lightning strike on 9 January 2003 and burned in Western Australia until 11 January 2003. The fire burned quickly through dry eucalypt forest of varying ages, propagating the furthest on 10 January 2003. Further background information is contained in Johnston et al. (2008).

The fire was simulated for a period of 21 hours starting on 10 January 2003.

7.2 Model Parameters

DATA TYPE	DATA SOURCE
Meteorological Data Used	Bickley AWS, ID: 009240, Lat/Long: -32.01, 116.14, Elevation: 384 m
Other Available Meteorological Data	Karnet AWS, Jandakot AWS and Dwellingup AWS
Land Use Classification	CLUM for data, initialisation model in Appendix A.1 was used for classification grid mapping
Topography	GA 30m raster (AHD)
Curing Level	Constant value of 80% was assumed based on time of year
Fuel Loads	A map of fuel ages in the region of the fire was sourced from Johnston et al. (2008) which was extracted and implemented in the simulation. Growth curves were then used to estimate fuel hazard scores.
Initial Fire for Simulation	Assumed to be at 116.295 E, 32.375 S with a radius of 310 m at 08:00 on 10 January 2003, based on Johnston et al (2008)
Simulation End Time	05:00 on 11 January 2003, based on Johnston et al (2008)
Output Comparison	Satellite imagery of the burn scar, Landsat 7 image LE71120822003036EDC00

7.3 Results and Discussion

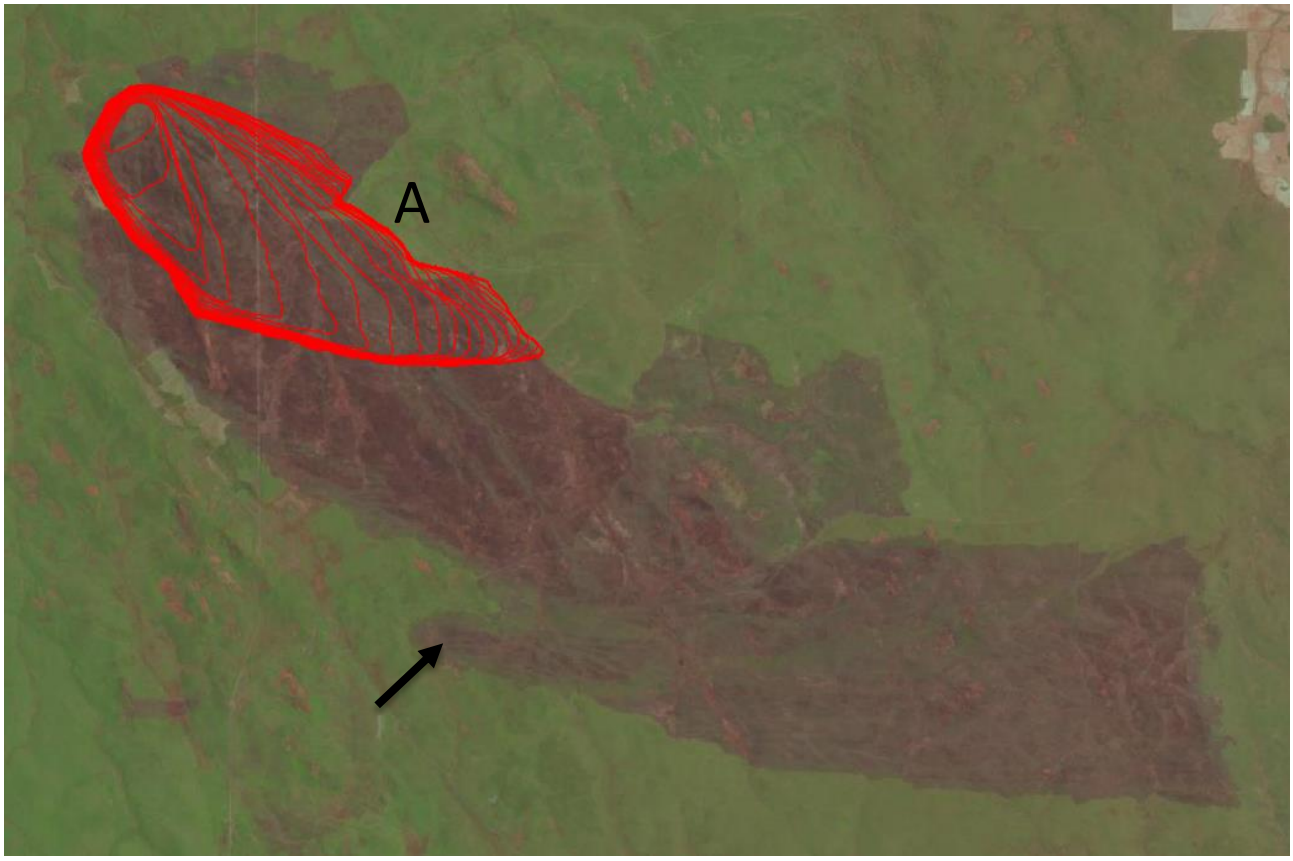

Figure 6 – Hourly isochrones of Mt Cooke simulation shown in red. First isochrone at 09:00 10 January 2003, last at 05:00 January 11. Isochrones are superimposed over a Landsat 7 image of the region taken on the 5th February 2003. The burn scar is visible as the dark brown region.

The Mount Cooke case provided the poorest match out of the test cases to the final observed fire extent, with a significant under prediction of the burned area (see Figure 6). This may be due to the following factors:

1. A spotting model was not included in the simulation. It was reported that significant spotting of 1-2km and even up to 5km occurred during the day of January 10 (Johnston *et al.* 2008). One such breakout from a spot fire can be seen on the satellite image (Figure 6, marked with an arrow).
2. Unmodified weather data from the Bickley AWS was used. This likely resulted in higher relative humidity, higher fuel moisture levels, and hence lower spread rates than were actually achieved. The wind direction in the first hour or so is also likely to have been south-westerly rather than south-easterly. Other simulations of this fire modified the weather data, including increasing the applied wind speed in order to obtain a similar burn area (Johnston *et al.* 2008).

To attempt to better correlate with actual fire observations, adjustments could be made to the input weather data including increasing the wind speed, modifying the wind direction and decreasing the relative humidity. The inclusion of a calibrated and published spotting model for the fuel type would also improve the simulation to match the actual fire better.

There was a slight over prediction of fire spread into the one year old fuels (area 'A'). This is likely due to the following reasons:

1. The youngest fuels tested in Gould *et al*. (2011) to develop fuel growth curves for low and tall shrub were 16 and 23 months respectively, and that the effects of very young fuels on fire spread rate were not accurately captured.
2. A property of the VESTA dry eucalypt model is that a forest which has just been burned (with fuel hazard scores of zero) is still predicted to propagate fire at a minimum spread rate given by the fuel moisture coefficient. This is perhaps a limitation of the model which could be improved upon for very young fuels.

To attempt to better correlate with actual fire observations, adjustments could be made to the one year old fuel in various sensitivity analyses.

8 Wangary Case

8.1 Background

The Wangary bushfire started on 10 January 2005 and burned in South Australia until 12 January 2003. The fire broke out from swamplands on 11 January 2005 and spread the fastest and burned the largest area on that day. Further background information is contained in Gould (2005).

The fire was simulated for a period of just over 14 hours starting on 11 January 2005.

8.2 Model Parameters

DATA TYPE	DATA SOURCE
Meteorological Data Used	1. North Shields (Port Lincoln) AWS*, ID: 018192, Lat/Long: -34.60, 135.88, Elevation: 28 m 2. Coulta (Coles Point) AWS, ID: 018191, Lat/Long: -34.37, 135.37, Elevation: 28 m 3. BoM ACCESS gridded data from Fawcett (2013)
Other Available Meteorological Data	None identified
Land Use Classification	CLUM for data, initialisation model in Appendix A.1 was used for classification grid mapping
Topography	GA 30m raster (AHD)
Curing Level	Constant value of 100% was assumed based on time of year
Fuel Loads	A constant fuel age of 10 years was assumed for the simulation. Fuel hazard scores were then estimated from growth curves.
Initial Fire for Simulation	A shapefile of the reconstructed fire at the end of 10 January 2005 was defined as un-burnable (already burned) while several breakout fires were modelled, the first starting at 09:51 on 11 January 2005 (Gould 2005).
Simulation End Time	00:00 on 12 January 2005 based on Gould (2005)
Output Comparison	Observed / reconstructed fire front at 00:00 on 12 January 2005 (Gould 2005)

* It should be noted that there is no publically available data from the North Shields AWS for a large portion of the fire duration. This data was, however, captured by BoM and has been privately supplied to us in a raw format with a 10 minute data capture period. The raw data was different to the publically available AWS data:

- Raw wind speed was recorded in knots. This was converted into km/h for the simulations.
- Percentage relative humidity was not recorded. This was calculated from the raw surface temperature t and dew point d in degrees Celsius using Eq. (3)[8].
- Wind direction was recorded to the nearest degree, not the nearest 10 degrees.

$$rh = 100 * 10^{7.591386\left(\frac{d}{d+240.7263} - \frac{t}{t+240.7263}\right)} \quad (3)$$

[8] Equation provided by Andrew Sullivan and was validated against complete data sets.

8.3 Results and Discussion

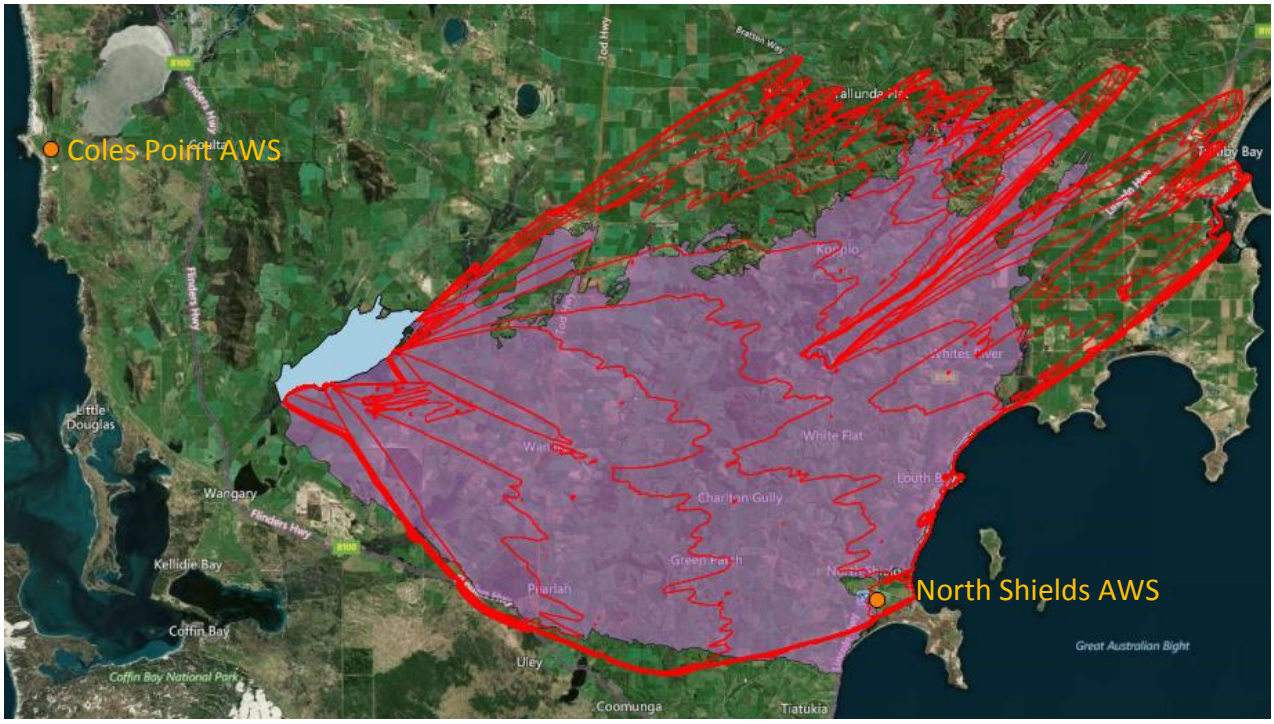

Figure 7 – Hourly isochrones of Wangary simulation shown in red. North Shields AWS data used for weather inputs. First isochrone at 10:51 11 January 2005. Overnight burn area shown in blue. Reconstructed fire at 00:00 12 January 2005 is shown in purple for comparison. Weather stations shown as orange circles.

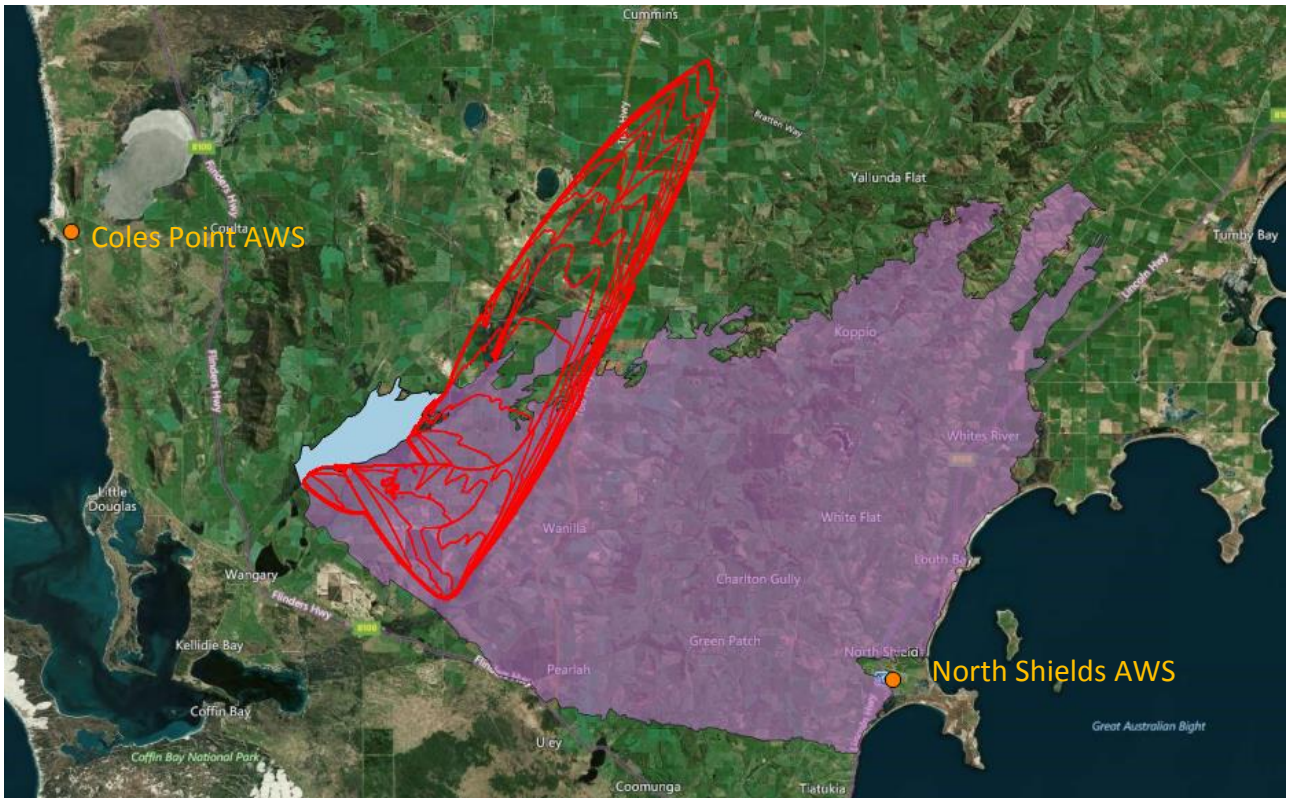

Figure 8 – Hourly isochrones of Wangary simulation shown in red. Coles Point AWS data used for weather inputs. First isochrone at 10:51 11 January 2005. Overnight burn area shown in blue. Reconstructed fire at 00:00 12 January 2005 is shown in purple for comparison. Weather stations shown as orange circles.

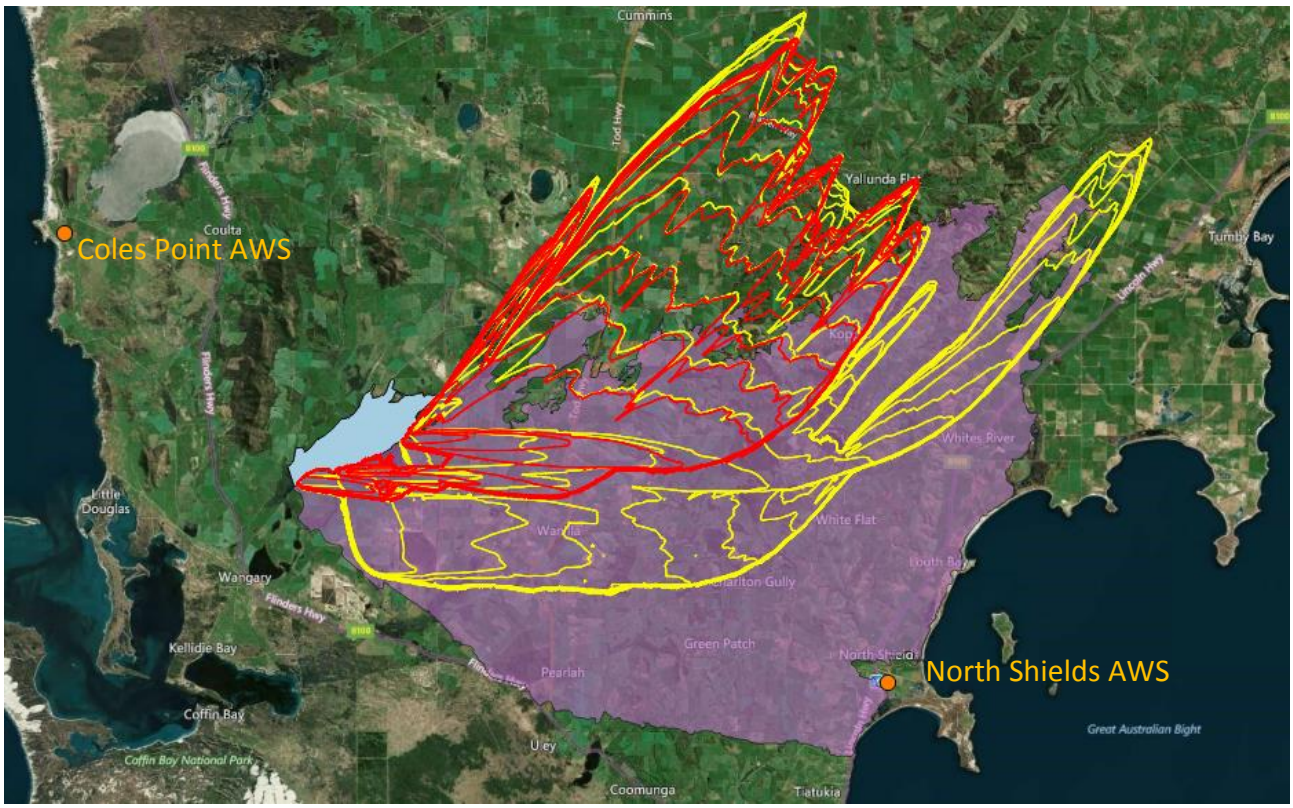

Figure 9 – Hourly isochrones of Wangary simulation. Raw gridded data used for weather inputs for red isochrones, one hour adjusted data used for yellow isochrones. First isochrone at 10:51 11 January 2005. Overnight burn area shown in blue. Reconstructed fire at 00:00 12 January 2005 is shown in purple for comparison.

The Wangary test case showed the greatest sensitivity to meteorological conditions of all the cases considered. While the rate of spread appeared to agree well with the observations, small differences in the timings of the wind change made great differences to the predicted fire perimeter. Figure 7 shows the simulation using North Shields AWS data, Figure 8 shows the simulation using Coles Point AWS data and Figure 9 shows the simulation using gridded weather model data.

8.3.1 North Shields meteorological data

The simulation using North Shields AWS data shows that the simulated fire generally matches the burn extent quite well, while slightly over predicting the burned regions in the North-East and North-West. Using the cut/grazed grass model instead of the undisturbed pasture grass model due to the large amount of farmlands in the area resulted in an even closer match to the actual burn area, however this analysis has not been included in this report. Use of a curing map and local topographic wind corrections may improve this match further.

8.3.2 Coles Point meteorological data

The simulation using Coles Point AWS data shows that the simulated fire does not spread far enough to the East before the wind change propagates the fire to the North-East. This is most likely due to the following reasons:

1. Unmodified weather data from the Coles Point AWS was used.

a. This possibly resulted in higher relative humidity, lower temperatures, and hence lower spread rates than were actually achieved, especially during the mid-afternoon when the wind was coming from the West.
b. Another issue is the wind direction and the timing of when the change comes through. Representing this with a single data point, many kilometres away from the active fire front, introduces significant error to when the fire changes direction.

8.3.3 Gridded meteorological data

The simulation which uses the raw gridded model data (red isochrones in Figure 9) shows that the simulated fire does not spread far enough to the South-East before the wind change propagates the fire to the East and then North-East. This is most likely due to the following reasons:

1. Unmodified model weather data was used.
    a. Figure 4 from Fawcett (2013) shows that the model weather data when the wind change occurs at the fire front is nearly an hour different from analysed data. This effectively removes the portion of the simulation which would propagate the fire to the South-East.

To attempt to better correlate with actual fire observations, adjustments can be made to the input weather data including modifying the start time by up to an hour in order to better match the analysed data of when the change hits the fire ground. This results in a better match (but not perfect) to the burn area as shown by the yellow isochrones in Figure 9. The inclusion of a topographic local wind corrector may also improve results.

The extent on the North-West flank for all simulations is greater than observed in the reconstruction. The cause appears to be the use of the ALUM classification for marshlands. In lieu of a known rate of spread model for these regions they would normally be treated as un-burnable. However, for this particular case, making these regions un-burnable prevents the observed initial breakouts from occurring. For these simulations the marshland regions were treated as grassland, which allowed the observed breakouts but gave increased spread rates through this regions, resulting in a larger final extent than observed. A general strategy for dealing with this issue is uncertain but could involve:

1. Manual modification of the classification data only within the area of the break out fires, keeping the other marshland areas defined as un-burnable. This is not a satisfactory solution as it would require manual tweaking of the classification layer for this particular case.
2. Development of a rate-of-spread model for marshlands. This could provide a balance between allowing the development of break out fires while reducing the spread through other marshlands. This would require further scientific investigation to develop the empirical rate of spread for marshlands.

9 Pickering Brook

9.1 Background

The Pickering Brook bushfire started from several deliberate ignitions on 15 and 16 January 2005 and burned in Western Australia until 25 January 2005. The fire burned through dry eucalypt forest of varying ages. Further background information is contained in Cheney (2010).

The fire was simulated for a period of 40 hours starting on 15 January 2005.

9.2 Model Parameters

DATA TYPE	DATA SOURCE
Meteorological Data Used	1. Bickley AWS, ID: 009240, Lat/Long: -32.01, 116.14, Elevation: 384 m 2. Wandering AWS, ID: 010917, Lat/Long: -32.67, 116.67, Elevation: 275 m
Other Available Meteorological Data	Perth Airport and Dwellingup
Land Use Classification	CLUM for data, initialisation model in Appendix A.1 was used for classification grid mapping
Topography	GA 30m raster (AHD)
Curing Level	Constant value of 80% was assumed based on time of year
Fuel Loads	A map of fuel ages in the region of the fire was sourced from Cheney (2010) which was extracted and implemented in the simulation. Growth curves were then used to estimate fuel hazard scores.
Initial Fire for Simulation	Fires 75, 76, 78, 79 and 80 were started with radii of 120 m on 15 and 16 January 2005, based on Cheney (2010). The first fire was started at 18:00 on 15 January 2005.
Simulation End Time	10:00 on 17 January 2005, based on Cheney (2010)
Output Comparison	Reconstructed fire perimeter isochrones from Cheney (2010)

9.3 Results and Discussion

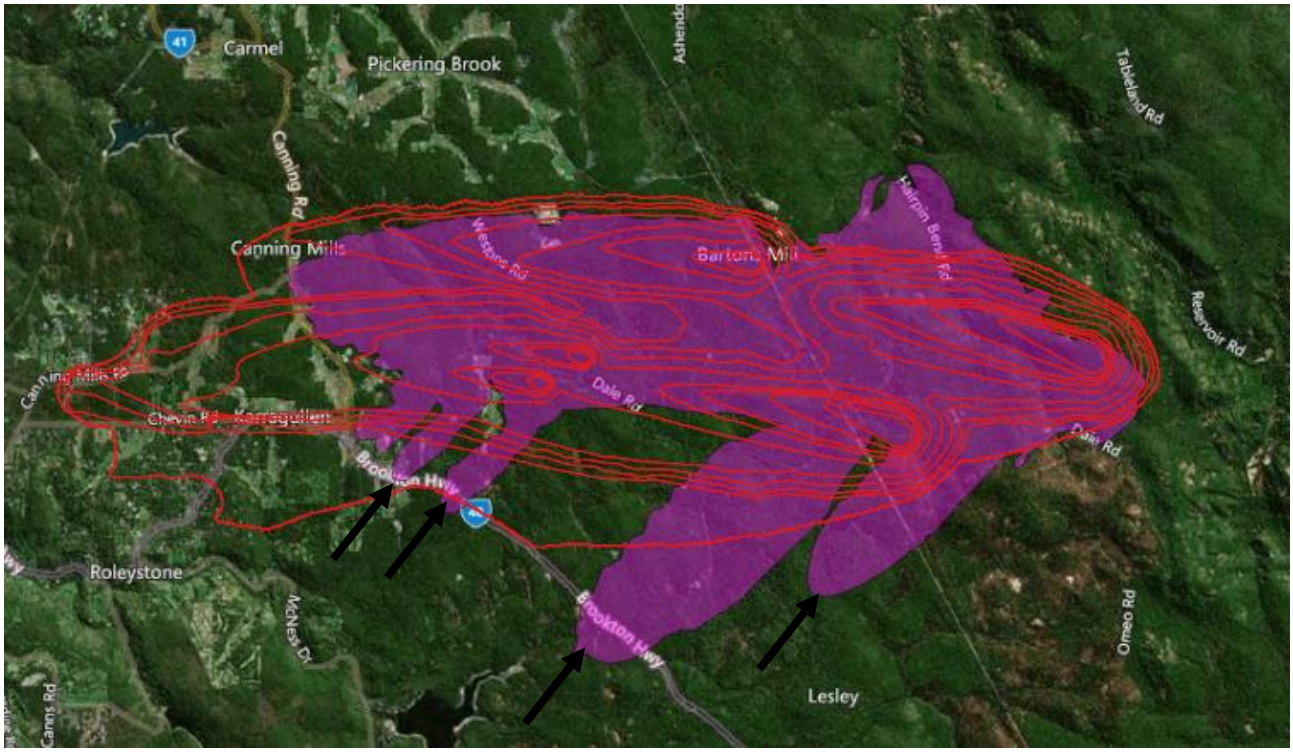

Figure 10 – Four-hourly isochrones of Pickering Brook simulation shown in red. Bickley AWS data used for weather inputs. First isochrone at 22:00 on 15 January, last isochrones at 10:00 on 17 January. Reconstructed fire at 10:00 January 17 shown in purple for comparison.

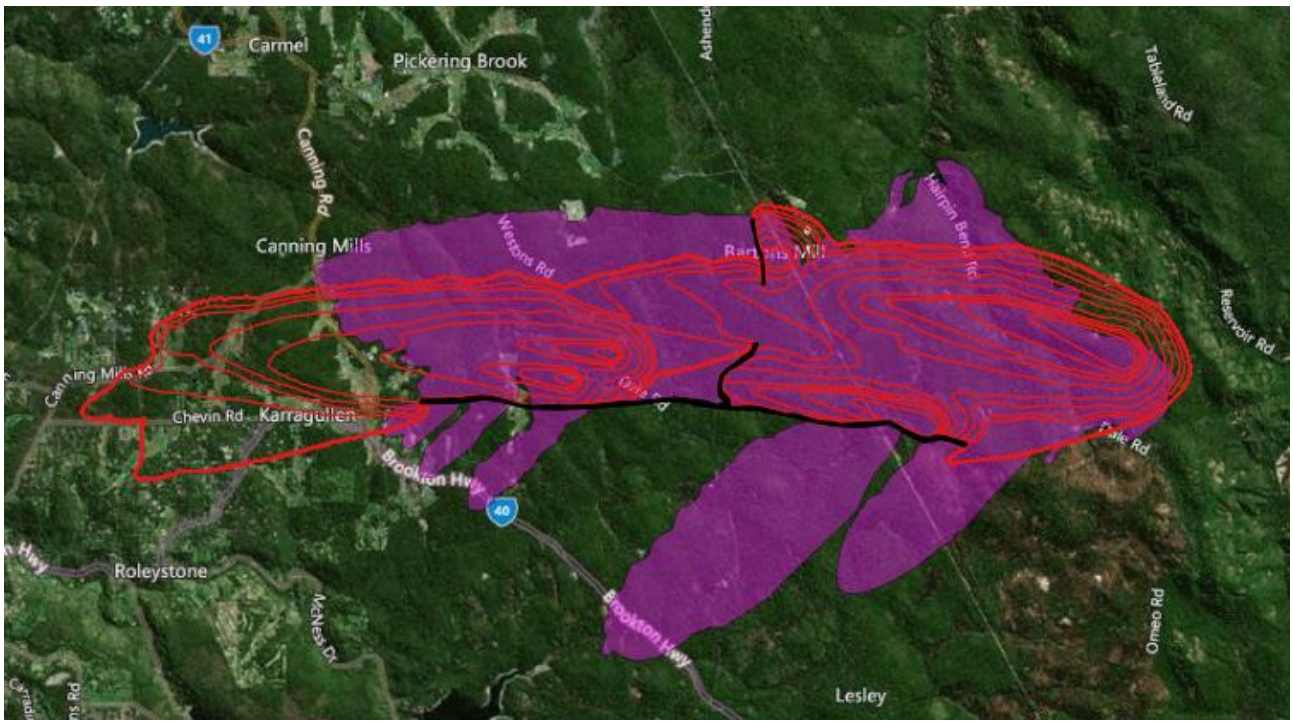

Figure 11 – Four-hourly isochrones of Pickering Brook simulation shown in red. Bickley AWS data used for weather inputs. First isochrone at 22:00 on 15 January, last isochrones at 10:00 on 17 January. Reconstructed fire at 10:00 January 17 shown in purple for comparison. Simulated control lines shown in black.

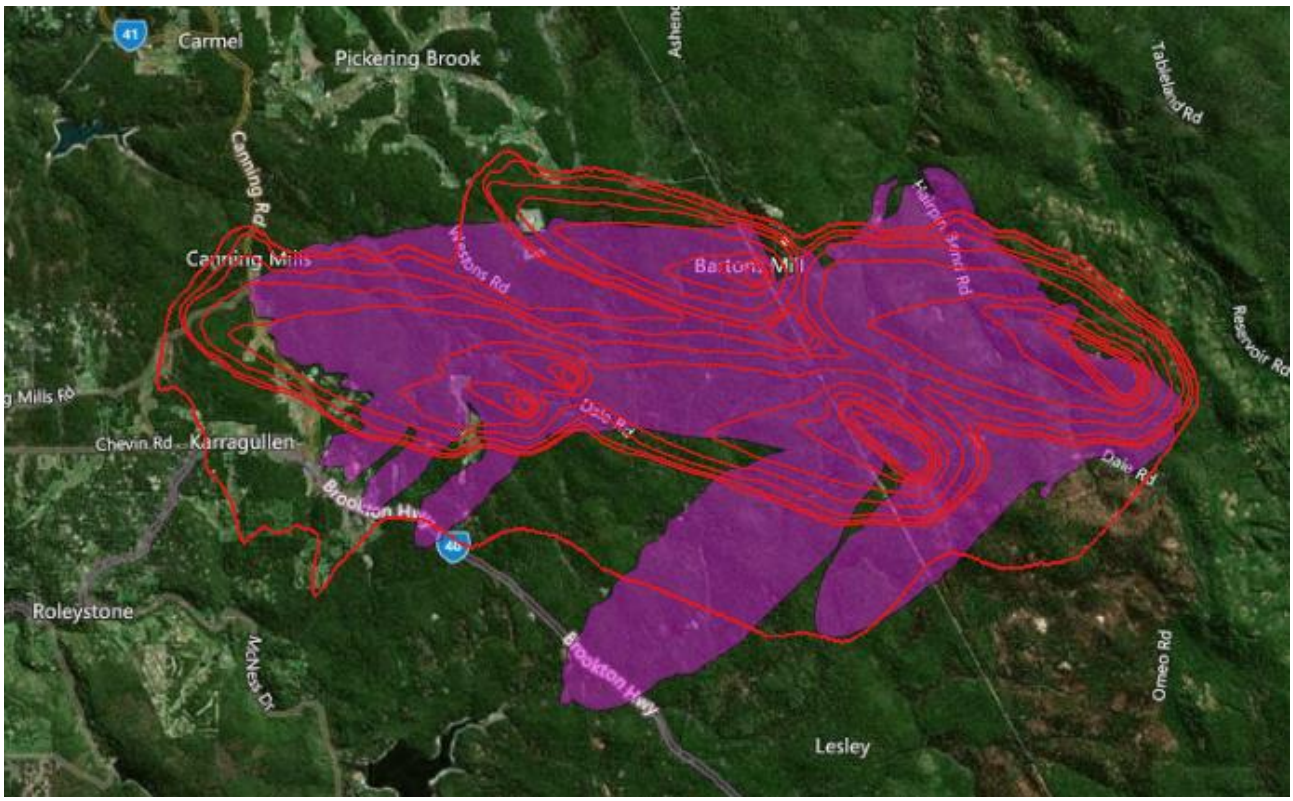

Figure 12 – Four-hourly isochrones of Pickering Brook simulation shown in red. Wandering AWS data used for weather inputs. First isochrone at 22:00 on 15 January, last isochrones at 10:00 on 17 January. Reconstructed fire at 10:00 January 17 shown in purple for comparison.

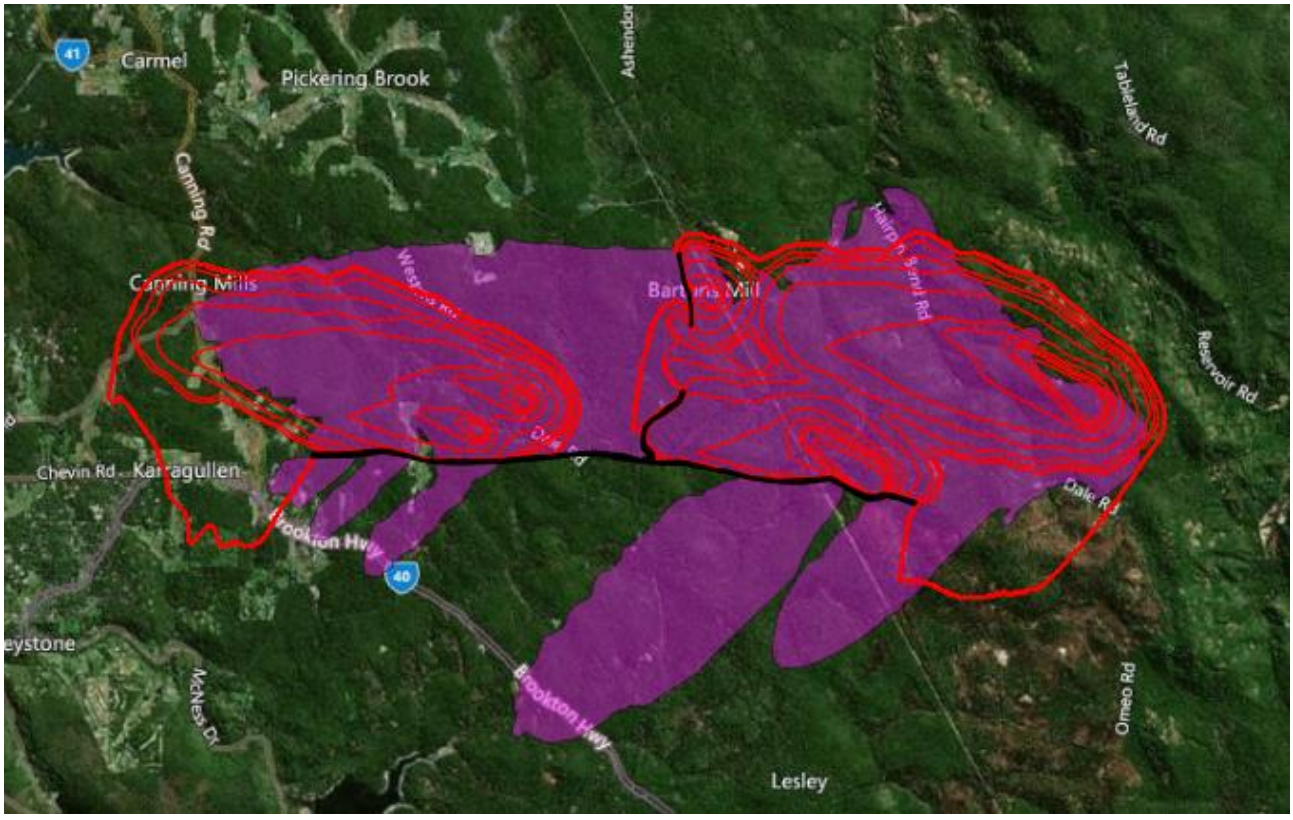

Figure 13 – Four-hourly isochrones of Pickering Brook simulation shown in red. Wandering AWS data used for weather inputs. First isochrone at 22:00 on 15 January, last isochrones at 10:00 on 17 January. Reconstructed fire at 10:00 January 17 shown in purple for comparison. Simulated control lines shown in black.

The Pickering Brook case provides a reasonable match over a long simulation duration but shows sensitivity to the meteorological data used. Figure 10 and Figure 11 shows the simulated fire using the Bickley AWS meteorological data both with and without containment lines respectively while Figure 12 and Figure 13 shows the simulated fire using the Wandering AWS meteorological data both with and without containment lines respectively.

This test case was also simulated using temporary containment lines employed during the early stages of the fire (Figure 7 from Cheney, 2010). The containment lines were implemented by creating thin polygons which were treated as un-burnable for the entire simulation.

9.3.1 Bickley meteorological data

Using the Bickley AWS data (approximately 10 km north of the fire) resulted in reasonable overall size and extent agreement with the reconstructed fire. The northern flank of the simulated fire matched the reconstruction well while the head fire was over predicted in the west. Several fire 'fingers' (arrows in Figure 10) were not predicted.

Implementing the containment lines caused the southern flank of the Bickley AWS simulation to match the reconstruction more closely (disregarding the breakouts of the fire to the south) while decreasing the overestimation of the fire extent to the west (Figure 11). The northern flank was under predicted as the northerly control line stopped the fire spreading in that direction.

9.3.2 Wandering meteorological data

Using the Wandering AWS data (approximately 75 km South-East of the fire) resulted in reasonable overall size and extent agreement with the reconstructed fire (Figure 12). The northern flank of the simulated fire matched slightly over predicted the reconstruction while the head fire was slightly over predicted in the west. The extent on the southern flank agreed reasonably well, although the 'fingers' were not well predicted.

Implementing the containment lines caused the southern flank of the Wandering AWS simulation provided a closer match to the reconstruction (again disregarding the breakouts of the fire to the south) while decreasing the overestimation of the fire extent to the west (Figure 13). However, the centre of the fires was under predicted as the north-south control line stopped the head fire spreading to the east, preventing the eastern and western fires from joining.

Differences between the simulations and recorded fire extents for both cases may be due to the following factors:

1. Several temporary control lines and suppression attempts were not modelled. These slowed and temporarily halted the progression of both the west travelling head fire and the southern flank of the fire. Point break outs occurred at the southern flank causing the 'finger' effect shown in the reconstructed isochrones (Cheney 2010).
2. A spotting model was not included in the simulation. It was reported that significant spotting of up to 1km occurred on January 15 and 16 (Cheney 2010).

3. Unmodified weather data was used. The wind data is likely to have not matched the actual conditions on the fire ground.

To attempt to better correlate with actual fire observations, adjustments could be made to the input weather data including modifying the wind direction, possibly combining the weather data from multiple weather stations. Modelling suppression attempts as well as temporary containment lines would improve the simulation further. The inclusion of a calibrated and published spotting model for the fuel type would also improve the simulation to match the actual fire better.

Although the inclusion of the control lines made the simulation perform better at the southern flank, the simulation performed worse in the central and northern areas. The inclusion of mid-range spotting may provide a better match to the reconstruction as the fires could jump over the north-south control lines. Treating the control lines as completely un-burnable also caused the simulation to become very sensitive to the wind direction in the early and middle stages of the fire. A slight change in wind direction could cause the fire to spread through the gap in control lines significantly earlier, increasing the burned area in the centre and north of the fire.

10 Ongoing Development

10.1 Input Data Limitations

Input data limitations can be a large source of error in wildfire models and predictions. Limitations often come in the form of incomplete input data for fuel classification maps, curing maps, fuel age or fuel load maps. Furthermore, on site meteorological data may be unavailable, limited or inaccurate. The largest errors are introduced into fire simulations from incorrect fuel classifications and incorrect local wind data.

Fuel classifications for this study have been taken from CLUM and TASVEG datasets as described in Section 2.3. Effort was made in mapping fuel classifications to the most appropriate spread rate model, however mapping to only the handful of spread rates used can introduce error into the overall rate of spread. This limitation can be minimised in the following ways:

1. Sourcing the most up to date and highest resolution land classification data. State specific data may be more specific and applicable in some cases compared to national data sets.
2. Regularly review the mapping from land classification to spread rate model especially as new spread rate models are developed and validated for new vegetation types.

Meteorological data for this study was taken from weather station data as well as gridded NetCDF model data. Using a single value for the wind speed and direction for the entire fire can introduce significant error, especially if this data is taken from a weather station tens of kilometres away. This limitation can be minimised in the following ways:

1. Sourcing and using validated high resolution weather data when available.
2. Using a model for down sampling and correcting wind flow over topography. This model in the Spark framework is currently undergoing testing and validation, and was not used in the current version of this study.
3. Using a model to adjust weather data based on the location of the fire relative to the weather station, and the wind speed and direction. This is currently undergoing development.
4. Ensemble simulations could be utilised within the framework with error estimations for weather variables such as wind direction and speed could be used in order to predict a probability map of where the fire will spread, rather than just a single prediction.

10.2 Fire spread modelling

Future developments of the spread model currently under active research may improve the predictive ability of the model in some areas. Some of these developments include:

1. Time varying moisture content models – this can be implemented in the current framework but was not included in this study.
    a. Possibly adding solar radiation model as an input to the fuel moisture content models

2. Lapse rate of varying temperature with elevation – this can be implemented in the current framework but was not included in this study.
3. A published and calibrated spotting model – research is required.
4. A greater understanding of wind and slope interaction – research is required.
5. New rate-of-spread models for different vegetation types – research is required. Any number of spread rate models can be implemented in the current framework.
6. Self-extinguishing of fires – research and development is required.
7. Fire suppression attempts – historical suppression data is required.
8. Topographic fuel load adjustment – research is required.

Appendix A Classification Initialisation Models

This Appendix contains the initialisation models for generating vegetation classification layers.

A.1 ALUM Classifications

For the Mount Cooke, Kilmore East, Wangary, Pickering Brook and Lithgow simulations, the ALUM classifications were used to generate the classification layer from the CLUM data based on the following initialisation model:

```
// Convert ALUM classification values to fuel types
const int main_class = (int)floor((REAL)class/100.0);
const int sub_class = (int)floor((REAL)class/10.0);


if (class == 650) {

  // Wetlands, mapped to grassland
  class = 1;

} else if (main_class == 6) {

  // Water
  class = 0;

} else if (main_class == 1 || sub_class == 22 || sub_class == 31 ||
sub_class == 41) {

  // Forest
  class = 2;

} else if (sub_class == 21 || main_class == 3 || main_class == 4) {

  // Grassland
  class = 1;

} else if (main_class == 5) {

  // Urban
  class = 3;

} else {

  // Default is un-burnable
  class = 0;

}
```

A.2 TASVEG

For the Giblin River and Forcett-Dunalley simulations, the TASVEG dataset was used to generate the classification layer. The following code was used in QGIS to convert the three letter vegetation codes into numbers:

```
CASE

WHEN regexp_match( VEGCODE,'^A') THEN 1
WHEN regexp_match( VEGCODE,'^D') THEN 2
WHEN regexp_match( VEGCODE,'^F') THEN 3
WHEN regexp_match( VEGCODE,'^G') THEN 4
WHEN regexp_match( VEGCODE,'^H') THEN 5
WHEN regexp_match( VEGCODE,'^M') THEN 6
WHEN regexp_match( VEGCODE,'^N') THEN 7
WHEN regexp_match( VEGCODE,'^O') THEN 8
WHEN regexp_match( VEGCODE,'^R') THEN 9
WHEN regexp_match( VEGCODE,'^S') THEN 10
WHEN regexp_match( VEGCODE,'^W') THEN 11

END
```

The classification grid was then generated using on the following initialisation model:

```
if (class == 1 || class == 5 || class == 8 || class == 9) {

  // Water (O), wetlands (A), highlands (H), rainforest (R)
  class = 0;

} else if (class == 2) {

  // Dry eucalypt (D)
  class = 2;

} else if (class == 4) {

  // Grassland (G)
  class = 1;

} else if (class == 3) {

  // Urban (F)
  class = 3;

} else if (class == 6 || class == 7 || class == 10) {

  // Moorland (M), non-eucalypt (N), scrub (S)
  class = 4;

} else if (class == 11) {

  // Wet eucalypt (W)
  class = 5;

} else {

  // Default is un-burnable
  class = 0;

}
```

References

Cheney et al. (1998) Prediction of fire spread in grasslands. International Journal of Wildland Fire 8, 1-15.

Cheney (2010) Fire behaviour during the Pickering Brook wildfire, January 2005 (Perth Hills Fires 71 – 80). Conservation Science Western Australia 7 (3): 451 - 468

Cruz, M.G., Sullivan, A.L., Gould, J.S., Sims, N.C., Bannister, A.J., Hollis, J.J., Hurley, R.J. (2012). *Anatomy of a catastrophic wildfire: The Black Saturday Kilmore East fire in Victoria, Australia*. Forest Ecology and Management 284, 269-285.

Cruz et al. (2015a) Effects of curing on grassfires: II. Effect of grass senescence on the rate of fire spread. International Journal of Wildland Fire 24, 838-848.

Cruz et al. (2015b) A guide to rate of fire spread models for Australian vegetation. CSIRO Land and Water Flagship, Canberra, ACT and AFAC, Melbourne, Vic, 123pp.

Fawcett et al. (2013) The Eyre Peninsula Fire of 11 January 2005: an ACCESS case study. (L.J.Wright (Ed) 2013, Proceedings of Bushfire CRC & AFAC 2013 Conference Research Forum, 2 September 2013, Melbourne Australia, Bushfire CRC)

Gould (2005) Development of Bushfire Spread of the Wangary Fire 10th and 11th January 2005 Lower Eyre Peninsula South Australia. Preliminary report to South Australia Coroner's Office and South Australia Country Fire Service. Revision 16 November 2005.

Gould et al. (2007) Field guide: Fuel assessment and fire behaviour prediction in dry eucalypt forest. Interim edition, CSIRO Publishing, Collingwood, Vic.

Gould et al (2011) Quantifying fine fuel dynamics and structure in dry eucalypt forest (Eucalyptus marginata) in Western Australia for fire management, Forest Ecology and Management 262 (2011) 531–546.

Johnston et al. (2008) Efficient simulation of wildfire spread on an irregular grid, International Journal of Wildland Fire, 17, 614-627.

Marsden-Smedley (2014), Tasmanian Wildfires January-February 2013: Forcett-Dunalley, Repulse, Bicheno, Giblin River, Montumana, Molesworth and Gretna

Matthews et al. (2010) Simple models for predicting dead fuel moisture in eucalyptus forests. International Journal of Wildland Fire 19, 1-9.

McArthur (1966) Weather and grassland fire behaviour. Commonwealth Department of National Development. Forestry and Timber Bureau, Leaflet 100, Canberra, ACT. 23 pp.

McArthur (1967) Fire behaviour in eucalypt forest. Commonwealth Department of National Development. Forestry and Timber Bureau, Leaflet No. 107, Canberra, ACT. 36 pp.

Schapel (2008) INQUEST INTO THE DEATHS OF STAR ELLEN BORLASE, JACK MORLEY BORLASE, HELEN KALD CASTLE, JUDITH MAUD GRIFFITH, JODY MARIA KAY, GRAHAM JOSEPH

RUSSELL, ZOE RUSSELL-KAY, TRENT ALAN MURNANE AND NEIL GEORGE RICHARDSON, Inquest conducted by Mr Anthony Schapel, Deputy State Coroner, South Australia. 2008.

Sharples (2008) Review of formal methodologies for wind-slope correction of wildfire rate of spread. International Journal of Wildland Fire 2008, 17, 179-193.

Sullivan et al. (2014) A downslope fire spread correction factor based on landscape-scale fire behaviour. Environmental Modelling and Software 62, 153-163.

Viney (1992) Modelling fine fuel moisture. University of New South Wales, University College, Department of Mathematics, Ph.D. Thesis, Canberra, ACT. 137 pp.

Viney and Hatton (1989) Assessment of existing fine fuel moisture models applied to Eucalyptus litter. Australian Forestry, 52, 82-93.

CONTACT US

t 1300 363 400
+61 3 9545 2176
e csiroenquiries@csiro.au
w www.csiro.au

AT CSIRO, WE DO THE EXTRAORDINARY EVERY DAY

We innovate for tomorrow and help improve today – for our customers, all Australians and the world.

Our innovations contribute billions of dollars to the Australian economy every year. As the largest patent holder in the nation, our vast wealth of intellectual property has led to more than 150 spin-off companies.

With more than 5,000 experts and a burning desire to get things done, we are Australia's catalyst for innovation.

CSIRO. WE IMAGINE. WE COLLABORATE. WE INNOVATE.

FOR FURTHER INFORMATION

Data61
James Hilton
t +61 0 0000 0000
e James.Hilton@data61.csiro.au
w https://research.csiro.au/spark/

Insert Business Unit name
Insert contact name
t +61 0 0000 0000
e first.last@csiro.au
w www.csiro.au/businessunit

Insert Business Unit name
Insert contact name
t +61 0 0000 0000
e first.last@csiro.au
w www.csiro.au/businessunit